2. Fundamentals

In the first part of the chapter fundamental theoretical and technical fundamentals of the used analytical instruments will be described.
In the second part of this chapter the substrate and the investigated organic molecules are introduced.

2.1. Scanning tunneling microscopy

The scanning tunneling microscope was invented by Gerd Binnig and Heinrich Rohrer in 1980. After the introduction into the scientific community in 1982 the outstanding capabilities of the method became clear since STM made it possible for the first time to analyze the topography and electronic structure of metal and semiconductor surfaces with atomic resolution in real space.[20] In 1983 the elucidation of the Si(111) 7x7 reconstruction proved to be the first scientific success of STM.[21] The importance and potential of scanning tunneling microscopy was underlined when Binnig and Rohrer received the Nobel Prize in Physics in 1986 for their invention. Nowadays STM remains an essential method for surface science. The operation principle of an STM is based on scanning a surface with a tip in close proximity and utilizing the resulting tunneling current for imaging and/or spectroscopy. The tunneling current is a pure quantum mechanical effect which will be explained in the next section.

2.1.1. The tunnel effect

In classic Newtonian dynamics a body cannot overcome or penetrate a potential wall that is higher than its energy (potential and kinetic). However, going from the macroscopic to the microscopic world Newton's laws of motion do not apply to certain processes. On the microscopic scale, for example for electrons, quantum mechanics has to be considered. In quantum mechanics the particle hitting the potential wall is actually able to penetrate this barrier with a certain probability. This pure quantum mechanical phenomenon is referred as tunneling effect.
In order to understand this effect some basic principles of quantum mechanics have to be introduced. Opposed to assigning a definite location and momentum to a body as in Newtonian dynamics, in quantum mechanics the state of a system like e.g. a photon or electron is defined by a wave function Ψ.[22] While the wave function itself

M. Lepper, *Insights into the Adsorption Behavior of a Prototype Functional Molecule,*
BestMasters, DOI 10.1007/978-3-658-11047-5_2, © Springer Fachmedien Wiesbaden 2015

has no physical meaning the square of its amplitude Ψ^2 at a certain point gives the probability of finding the particle at this position.

The description of quantum mechanical states and processes is done by combining wave functions and corresponding operators. The Schrödinger equation which is the most fundamental equation of quantum mechanics defines the total energy of a system E using the Hamilton operator $\hat{\mathrm{H}}$.

$$\hat{\mathrm{H}}\Psi = E\Psi$$

It is known that for the case of a 'particle in a box' the Schrödinger equation shows that the particle has some probability to be found outside the potential well.[23-24] For illustration and explanation of the tunnel effect a simple model system quite similar to the 'particle in a box' can be used (Figure 2.1.1-1). In this one-dimensional model the particle is travelling with a kinetic energy E_0 in a potential free region A and hits a potential barrier B of height $V_0 > E_0$ and width d. With a probability T the particle tunnels through the barrier into the potential free region C.

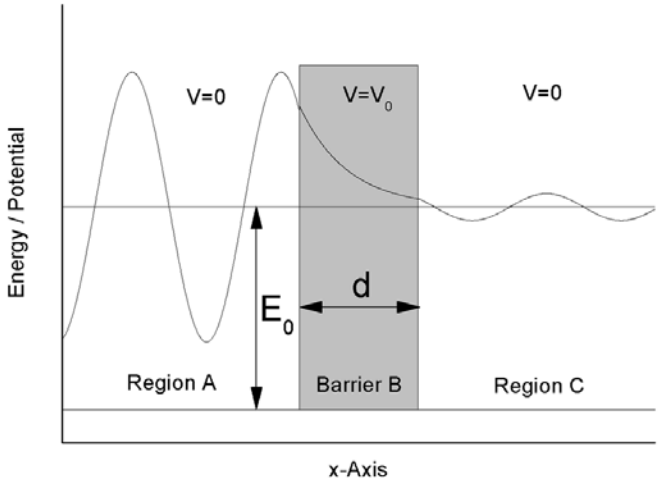

Figure 2.1.1-1 Scheme of a one–dimensional tunneling barrier.[24]

Using the Schrödinger equation it is quite easy to formulate the wave functions for the different regions in the model.
In region A the particle has the highest amplitude and thus maximum probability to be found. The wave function resembles an oscillation:

$$\Psi(x) = \Psi(0)\, e^{ix\sqrt{\frac{2m(E_0-V)}{\hbar^2}}}$$

Within the barrier (region B) the amplitude of the wave function and thus the probabildity (Ψ^2) of the particle to be found at the given position are decreasing exponentially. In the following equation Δx equals the distance into the barrier:

$$\Psi(\Delta x) = \Psi(0)\, e^{-\Delta x\sqrt{\frac{2m(V_o-E_o)}{\hbar^2}}}$$

In region C the maximum amplitude is reduced however the probability to find the particle in this region is not zero:

$$\Psi(x) = \Psi'(0)\, e^{ix\sqrt{\frac{2m(E_0-V)}{\hbar^2}}}$$

The tunneling probability can be then put in the following equation:

$$T = \frac{4E_0(V_o - E_o)}{V_0^2}\, e^{-\frac{2d}{\hbar}\sqrt{2m(V_o-E_o)}}$$

Thus the probability depends on the energy E_0 and the mass m of the particle as well as the height V_0 and the width d of the potential barrier. It should be noted that even though the square of the wave function decreases, the wavelength resembling the energy of the particle remains the same after tunneling.

The principle of the simple model system shown above can be transferred to explain the tunneling process in STM (see figure 2.1.1-2). In this figure the sample represents the potential free region A while the other potential free region C is related to the tip. In principle a tunneling current can be measured without applying a bias voltage (eU). However in order to maintain the difference between Fermi energies and to address different orbitals for the tunneling process, generally a bias voltage is applied. It has to be noted that in this thesis the sign of the bias voltage denotes the polarity of the sample. Thus negative bias means tunneling from the sample to the tip and positive bias tunneling in the opposite direction.

Furthermore in the thesis at hand different adjectives describing the magnitude of bias voltage will be used. For definition these adjectives will relate to the absolute value of the voltage. For example bias voltages like ±200 mV will be referred as ‘small’, while ±1000 mV is considered ‘large’.

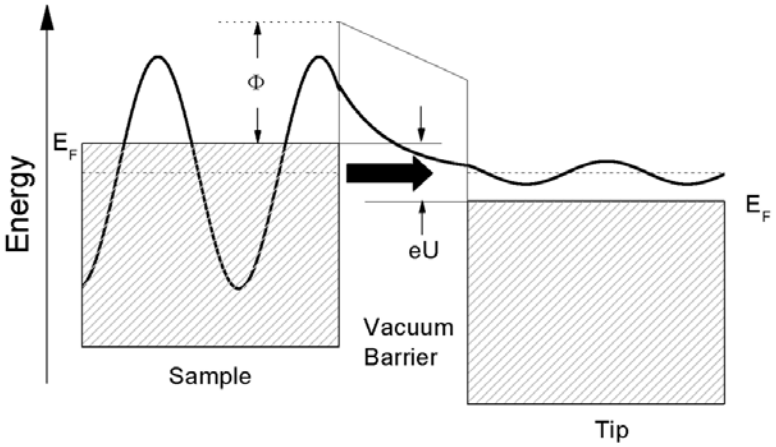

Figure 2.1.1-2 Schematic of the theoretical principle of STM. Modified from [25].

Coming back to figure 2.1.1-2, the barrier height is approximately the mean work function Φ of tip and sample while *d* is the width of the barrier. The grey shaded areas resemble the occupied states of sample and tip.

$$\Phi = \frac{1}{2}(\Phi_{sample} + \Phi_{tip})$$

For STM measurements a bias voltage (*eU*) is applied between tip and sample. The bias voltage (*eU*) yields an energy gradient by shifting the Fermi energies (E_F) of tip and sample. Thus in the case of figure 2.1.1-2 electrons from the occupied valence band of the sample can tunnel into the unoccupied conduction band of the tip.
This flow of electrons is the tunneling current *I* which depends exponentially on the sample to tip distance *d*.

$$I \propto U_{bias} \cdot \rho_s \cdot e^{-\frac{2d}{\hbar}\sqrt{2m\Phi}}$$

From this equation it can be derived that the tunneling current depends on the local density of states (LDOS) at the sample surface ρ_s and the tunneling bias U_{bias}. The LDOS is defined as number of electrons per unit volume per unit energy, at a certain point in space at a specific energy.[25]

The exponential dependence of the tunneling current on the sample to tip distance provides the high z-sensitivity of STM. Moreover the influence of the LDOS on the tunneling current supplies information about the electronic structure of the surface.

2.1.2. STM operation principle

The operation principle of a scanning tunneling microscope is illustrated in figure 2.1.2-1.

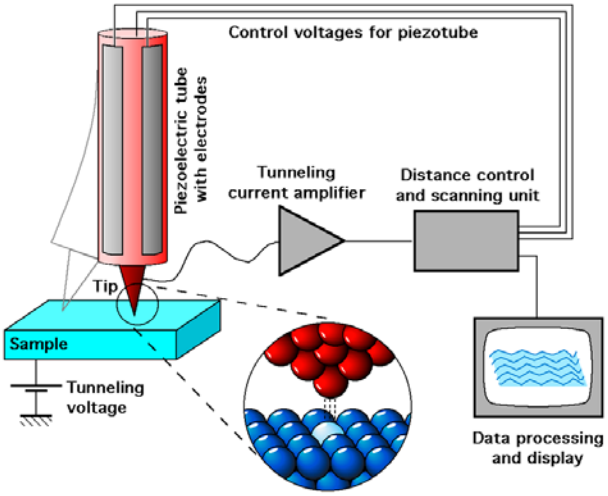

Figure 2.1.2-1 Schematic drawing of the operating principle of a scanning tunneling microscope.[26]

For an actual measurement a bias voltage between ±0.1 V and 3.0 V is applied and the sharp metallic tip is approached to the surface until a predetermined tunneling current is reached. The tip is then scanned over the surface at a distance in the nm regime and the corresponding tunneling current in the range of few pA to nA is

measured. Control of the tip position is accomplished by applying specific voltages at a piezoelectric scanning tube on which the tip is mounted.

In STM two different modes to gain information from the tunneling current can be distinguished. Figure 2.1.2-2 illustrates these two modes.

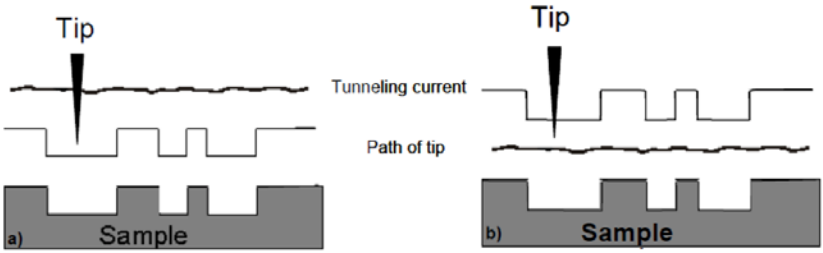

Figure 2.1.2-2 Comparison of the two STM operation modes: **a)** constant height mode (CHM) and **b)** constant current mode (CCM).[27]

In the constant current mode (CCM) the sample is scanned at a constant tunneling current. A constant value of the tunneling current is maintained by a feedback loop that measures and counteracts the deviation of the actual tunneling current from the current setpoint. Thus the vertical tip position is adjusted such that the actual tunneling current remains at the given set point. The changes of the vertical tip position can then be translated into a color coded image by the software. However, the scan speed of this mode is limited by the restricted reaction time of the feedback loop.

Another way of scanning the tip across the surface is the constant-height mode (CHM) in which the z-position of the scanner is not changed and the current is recorded as a function of its lateral position on the surface. Therefore it is not necessary to implement a feedback loop. Thus the CHM can be applied with higher scan speeds than the CCM. In contrast a disadvantage of the CHM is the limitation to flat surfaces as surface defects and irregularities can cause a crash of the tip.

In the thesis at hand the STM was operated exclusively in constant current mode.

2.1.3. Tersoff-Hamann theory and related concepts

The one dimensional model for the tunnel effect explains only the basic principles of scanning tunneling microscopy. However, more complicated issues like the influence of the tip structure and shape cannot be understood with this simple model. In 1983 Tersoff and Hamann published a first model based on time-dependent perturbation theory enabling the calculation of the tunneling current considering the tip constitution.[28-29] The tunneling current was found to be proportional to the surface local density of states (LDOS) which are projected in constant current mode STM images. For this model the tip is assumed to be hemispherical with a spherical or s-like potential as depicted in figure 2.1.3-1. However soon after publication the limitations of the model became clear since it was not able to explain the atomic resolution of various substrates.

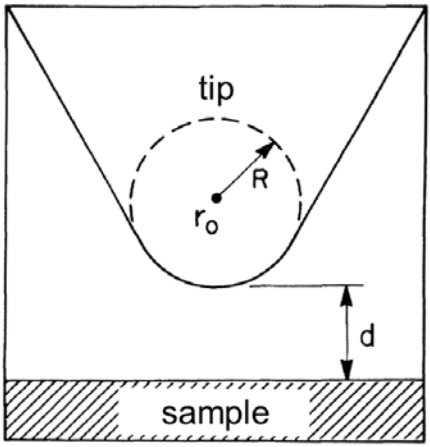

Figure 2.1.3-1 Spherical potential utilized by the Tersoff Hamann model to describe the tip state. Modified from [28].

Contemporary Baratoff proposed a model concerning the STM resolution of the Si(111) 7x7 reconstruction.[30] His model was based on a localized d_{z^2} orbital located at the apex of the applied tungsten tip.

The importance and existence of this d_{z^2} orbital was shown by 'first principle' calculations performed by Onishi et al. in 1989.[31] In 1991 Chen published the correspond-

ing theory focusing on the interaction between localized states of tip and sample (see figure 2.1.3-2).[32] The significance of this theory is that it not only explains the origin of atomic resolution but also the principle of improving the tip. Application of pulses and crashing the tip are supposed to produce localized surface states through which tunneling takes place.

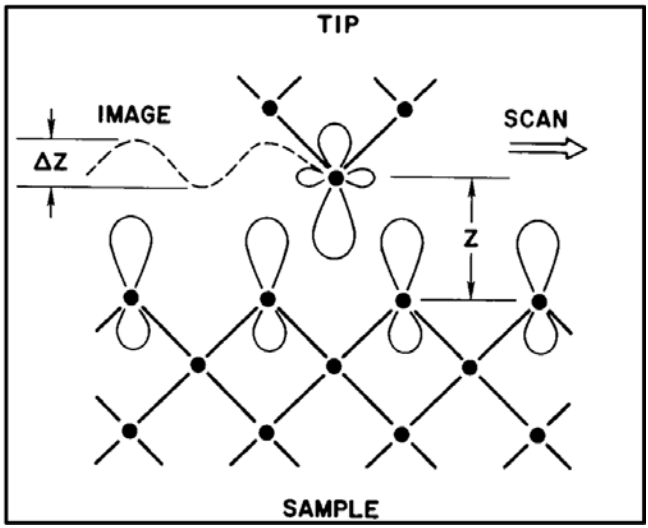

Figure 2.1.3-2 Illustration of the interactions between localized states of tip and sample.[32]

2.2. Quadrupole mass spectrometry

Today several mass spectrometry methods exist that dependent on different ionization processes and/or mass detection methods. Generally ionization and acceleration towards a mass filtering device take place in vacuum environment. The ionization process usually leads to characteristic fragments of the ionized molecule. This fragmentation can be used to determine the chemical composition and fragmentation behavior of the molecule.

After ionization and acceleration the particles of different mass and charge have to be separated according to their mass to charge ratio m/z and be detected. A typical mass spectrum is then an intensity spectrum of all possible mass to charge ratios of all fragments.

Figure 2.2-1 shows the working principle of a quadrupole mass filter. In a quadrupole mass spectrometer ion separation is accomplished by an oscillating electric quadrupole field. The quadrupole consists of four parallel rods where adjacent rods have opposite voltage polarity applied to them (see figure 2.2-1). The oscillating field is generated at the rods by a sum of constant DC voltage U and varying radio frequency (U_{rf} cos (ωt)), where ω = angular frequency of the radio frequency field. After the ionization in the source the ions are accelerated in a way that they travel parallel to the four rods. However for given DC and AC voltages, only ions of a certain mass to charge ratio pass through the quadrupole filter and all other ions are deflected from their original path. Thus by varying the oscillating frequency all possible *m*/*z* ratios can be obtained and a mass spectrum is received.

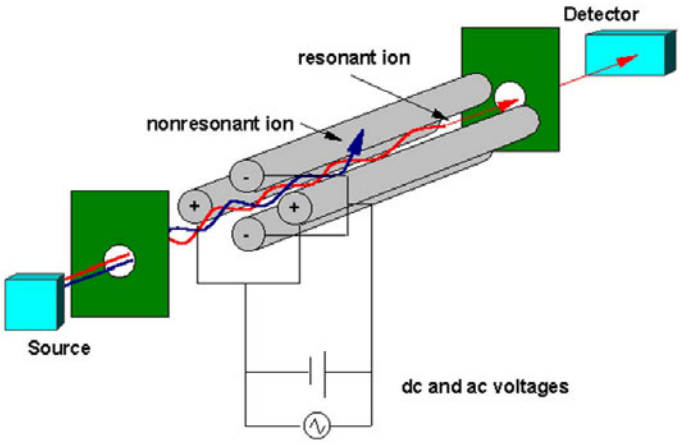

Figure 2.2-1 Setup of a quadrupole mass spectrometer.[33]

2.3. Substrate properties

The substrate used in the work at hand is a copper single crystal with a polished (111) surface. Table 2.3-1 shows an overview of several selected properties of copper.

properties	Cu
atomic number	29
relative atom mass	63,55
melting point	1084 °C
boiling point	2595 °C
electron configuration	[Ar] $3d^{10}$ $4s^{1}$
density	8,92 g/cm³
electronegativity	1,8 (Pauling)
electric conductivity (at 298K)	59,4 10^{6} S/m
atomic radius	128 pm
crystal structure	fcc
lattice constant	3,61 Å

Table 2.3-1 Physical properties of copper.[34]

Figure 2.3-1 a) shows the unit cell of the cubic face centered copper lattice with a lattice constant of 3.61 Å. The green planes in a) resemble the (111) surface.
Figure 2.3-1 b) presents a topview of the (111) surface from which it can be derived that Cu (111) is hexagonal close packed. The planes are orientated perpendicular to the space diagonal of the fcc lattice. Within one layer the Bravais lattice is hexagonal with a lattice constant of 2.55 Å. As it is known for hexagonal close packed lattices the layers follow an ABC stacking where every fourth layer is congruent to the first. The atoms of one layer fill the vacant spaces of the respective upper layer leading to dense packing. In figure 2.3-1 b) the arrows are used to emphasize the three-fold high symmetry axes of Cu (111). Similar arrows will be used in later chapters to indicate the substrate orientation.

http://www.springer.com/978-3-658-11046-8

Insights into the Adsorption Behavior of a Prototype Functional Molecule

A Scanning Tunneling Microscopy Study

Lepper, M.

2015, XI, 86 p. 41 illus., Softcover
ISBN: 978-3-658-11046-8